

Stimuli Mediated Ultrastable Radical Formation

Jade A. McCune¹, Moritz F. Kuehnel^{2,3}, Erwin Reisner² & Oren A. Scherman¹

¹*Melville Laboratory for Polymer Synthesis, Department of Chemistry, University of Cambridge, Lensfield Road, Cambridge CB2 1EW, UK.*

²*Christian Doppler Laboratory for Sustainable SynGas Chemistry, Department of Chemistry, University of Cambridge, Lensfield Road, Cambridge CB2 1EW, UK.*

³*Current Address: Department of Chemistry, Swansea University, Singleton Park, Swansea, SA2 8PP, UK.*

Organic radicals are reactive, often short-lived species typically formed through either the addition of a chemical reducing or oxidising agent or photochemical means. On account of their open-shell electronic structure they have attracted much attention based upon their magnetic properties and desirable spectroscopic behaviour. Redox sensitive molecules such as viologen (V) can undergo one-electron reductions to form radical species. These organic radicals hold significant potential in myriad applications but are limited as they are rapidly quenched by oxygen leading to short lifetimes in air. Using methyl viologen as an example, we show that the MV radical ($MV^{+\cdot}$) can be formed through electrochemical, chemical, photochemical and a novel thermal stimulus in various Deep Eutectic Solvents (DES) and was found to be exceptionally stable. Our report represents a unique approach to extend radical lifetimes in air without the use of a receptor or alteration of its chemical or electronic structure. The conductive properties of DES allowed for fabrication of an aerobic electrochromic

device based on MV through a straightforward, economical approach. The device was robust and stable, introducing a new manufacturing route for solution based, scalable, cost-effective production of switchable displays and devices.

The use of a stimulus to alter the structure and properties of redox-active molecules has been exploited across a wide range of chemistries. Redox-responsive systems are readily switched using electrochemical, chemical or, in some cases, photochemical stimuli. Redox systems are desirable as, unlike other responsive systems, a change in both the charge and spin state of the molecule occurs.¹ These systems have been utilised for many applications including drug delivery,² displays,³ electronic memory,⁴ batteries⁵ and tuneable materials.¹ Typical redox active molecules include metallocenes such as ferrocene and aromatic derivatives such as tetrathiafulvalene, naphthalene diimides and viologen derivatives.¹ Isolation and characterisation of organic radicals are often impeded by their instability and transient nature. To overcome this limitation encapsulation within receptors has been a common way to stabilise and prolong the lifetime of such species. This has been demonstrated elegantly for chemically reactive species,^{6–8} radical cations⁹ and anions.^{10–12} Of interest are dicationic viologen derivatives, which can undergo a one-electron reduction to form intensely coloured radical cations with chemical and electrochemical applications as electron mediators. These species are stable in the absence of any oxidising agent as the unpaired electron is delocalised across the π -system.¹³ However, in the presence of molecular O₂ their quenching is extremely rapid.¹⁴ The electrochromic behaviour of viologen derivatives, in particular the high optical contrast between redox states, has led to their application in electrochromic devices and displays. Companies have produced electrochromic devices based on viologen, including Genetex

who have produced a best-selling electrochromic mirror currently used in cars.¹³ Nevertheless, the poor dication solubility and short radical lifetime of MV in air has limited its applications within current commercial devices which instead use substituted or immobilised viologen derivatives requiring additional costly manufacturing steps. The use of receptors to stabilise MV radical cations has been reported. Kim and co-workers demonstrated enhanced stability upon encapsulation inside a macrocyclic host, cucurbit[n]uril.^{15,16} This concept was shown to be extended to the formation of 2D supramolecular organic frameworks.¹⁷ The formation a crystalline supramolecular complex between MV^{2+} and a bambusuril macrocycle was shown by Sindelar and co-workers.¹⁸ The crystals could undergo photoinduced electron transfer to form $MV^{+\cdot}$ radicals within the crystals, which were found to have a half-life of several hours in air. Recently, the encapsulation of MV^{2+} in a zeolite resulted in a photochromic material through electron transfer between the MV^{2+} and the anionic zeolite framework. The dense packing of MV^{2+} within the zeolite pores resulted in a short electron transfer pathway and thus photochromic behaviour in addition to stability of the radical state as the framework prevented contact with oxygen.¹⁹ Stoddart and co-workers have put significant research effort into constructing mechanically interlocked molecules based on MV^{2+} . The most exploited example is the formation of cyclobis(paraquat-p-phenylene) ($CBPQT^{4+}$), “blue box”, where two methyl viologen moieties are joined through a spacing bridge to form a box-like structure.²⁰ Although not air stable, it allows access to a more stable $MV^{+\cdot}$ radical species which can undergo molecular recognition to form charge transfer complexes, and extended structures such as rotaxanes²¹ and catenanes.^{22,23}

Deep Eutectic Solvents (DES) were first introduced by Abbott and co-workers in 2003 as a new

class of ionic liquids (ILs) composed of two non-symmetric components, which can undergo complexation.^{24,25} Typically, one component is a quaternary ammonium salt (commonly choline chloride, ChCl) and the other a metal salt or hydrogen bond donor (*e.g.* amide, alcohol or acid).^{26,27} The hydrogen bonding interactions that occur during complexation result in charge delocalisation and thus the melting point for the complex is lower than the individual melting points of the components. The precise organisation of the components upon complexation and the resulting liquid structure is not yet fully understood for all eutectic mixtures as the field is still in its infancy. Recent studies based upon computational and neutron scattering data probe the precise hydrogen bonding interactions and the bulk liquid structure for the most common DES, ChCl-urea (1:2).^{28,29} Reports on the nanostructure (dynamic molecular configuration) of DES,²⁸ in particular the effect of water upon it,³⁰ are also emerging.

While DES are not composed of discrete anionic and cationic species and have very different chemical properties to ILs, they do have similar physical properties such as low vapour pressure, non-flammability and a wide temperature range over which they remain liquid.^{26,27} Both DES and ILs are “tuneable” solvents as their properties can be altered for specific applications based upon selection of individual components with over 10^6 different combinations predicted.²⁶ In contrast to ILs, the preparation of DES is facile, non-toxic and inexpensive with many components produced annually on a multi-ton scale. DES applications to date have been based upon their excellent solubilising properties and mainly focused on areas such as electrodeposition³¹ but have also been used for synthesis of nanoparticles,³² gas adsorption³³ and as a solvation medium for traditional organic transformations.^{34,35}

Here we utilise the nanostructure of DES as a novel supramolecular confined environment to explore the redox properties of MV as an exemplar organic radical species and show stimuli-responsive behaviour towards electrochemical, chemical, photochemical and a novel thermal stimulus. In all cases, we observe the typically short-lived radical cation to be extremely persistent in DES even in oxygenated environments with drastically extended lifetimes of approximately 10^5 fold compared to water. Accessing a long-lived, air, light and heat stable redox-responsive radical under ambient aerobic conditions holds tremendous potential in areas including switchable displays and smart-windows. The persistence of $MV^{+\cdot}$ in DES negates bleaching and renders current efforts to improve solubility and write-erase efficiencies redundant. Moreover, in contrast to current technologies, our approach is economically and environmentally preferable using components already produced on a multi-tonne scale annually and requiring only solution-based processing methods.

Electrochemical switching. MV is a redox active molecule (Fig. 1A) that can undergo a one-electron reduction to form an intensely coloured blue solution (Fig. 1B). To determine how solvent nanostructure impacts redox behaviour of MV, we explored the electrochemical response of MV^{2+} in different DES. DES themselves are known to act as electrolytes³⁶ and therefore all measurements were undertaken using solutions of MV^{2+} in neat DES with all redox potentials given in reference to the hydroxymethylferroceninium/hydroxymethylferrocene redox couple (FcMeOH), serving as internal reference. Cyclic voltammetry in three typical DES, ChCl-urea, ChCl-ethylene glycol and ChCl-glycerol showed that MV^{2+} could undergo two consecutive one-electron reductions (Fig. 1C, S1) and both processes were fully reversible. Consecutive cycling between MV^{2+} , $MV^{+\cdot}$ and

MV⁰ was performed to demonstrate cycling stability, a key requirement for electrochromic and battery applications. Remarkably, all DES-MV solutions were found to be stable over 100 cycles with no change in the electrochemical response and no sign of MV degradation. This finding was particularly impressive as the measurements were performed in air without any degassing of the solutions. Such stability in air is unusual for radical cations such as MV^{+·}, which are highly reactive towards oxygen, and suggests stabilisation of MV^{+·} in DES environments.

Chemical switching. Switching between MV²⁺ and MV^{+·} using a chemical stimulus was investigated through monitoring the optical properties upon addition of different reducing agents (Fig. S2). A visible colour change from colourless to an intense blue was observed, indicating the formation of the MV^{+·} radical cation with a characteristic UV/vis spectrum ($\lambda_{max} = 399$ nm and 609 nm). To re-oxidise MV^{+·} to MV²⁺ solutions were bubbled with air to introduce O₂ into the system and quench the radical. When purged with air, the solution slowly returned to colourless which was associated with the loss of all absorption between 300-800 nm (Fig. 1D, S3).

Photochemical switching. MV²⁺ has shown photochromic behaviour in solution,³⁷ within films³⁸ and in the crystalline state^{18,38} leading to applications in photonic devices, erasable data storage systems and liquid crystals. The photochromic behaviour is reported to occur through photoinduced electron transfer between the counter anion and MV²⁺ cation.³⁸ Typically, this requires irradiation with middle UV light, however, using natural light as a stimulus is highly desirable for applications such as self-tinting windows.

The photochromism of MV in three different DES was probed using simulated solar light (AM

1.5G, 100 mW cm⁻²). Upon irradiation, the colourless MV²⁺ solution turned blue, indicative of MV^{•+} generation, which was confirmed by its characteristic absorbance in the UV/vis spectrum (Fig. S4). The radical was observed to originate at the interface of the solution with the incident light forming a blue layer that gradually grew into the solution over time (Supporting Video S1, Fig. 1E). Visualisation of this process in real time highlights the unique way in which the MV^{•+} species is held within the nanostructure of the DES. Remarkably, no difference was observed whether photoreduction experiments were performed under aerobic or anaerobic conditions. Moreover, the resulting MV^{•+} solutions were stable in air with measurements taken over several hours open to air without further irradiation showing no detectable loss of absorbance at 609 nm in the UV/vis spectrum. This suggested that the MV^{•+} was not being quenched by atmospheric O₂ indicating again that the DES have a stabilising effect.

It was found that a MV solution could undergo multiple cycles of photoirradiation and purging without any impact on performance (Fig. 1F). The rate of photochromic coloration could be tuned by varying the nature of the DES (Fig. 1G, S4). For alcohol-based DES (ChCl-ethylene glycol and ChCl-glycerol) the formation of MV^{•+} was faster compared to amide-based ChCl-urea DES under the same conditions. We postulate this is a result of the photoreduction mechanism as alcohols are known to rapidly quench the MV²⁺ excited state with formation of MV^{•+}.³⁹ The rate of MV^{•+} formation could be further controlled by varying the MV²⁺ concentration (Fig. S5). Decolouration of MV^{•+} solution was achieved by purging the solution with air (Fig. 1H, S6) with the rate of decolouration dependent on gas flow into the solutions (Fig. S7), all solutions reverted to colourless within 150 s.

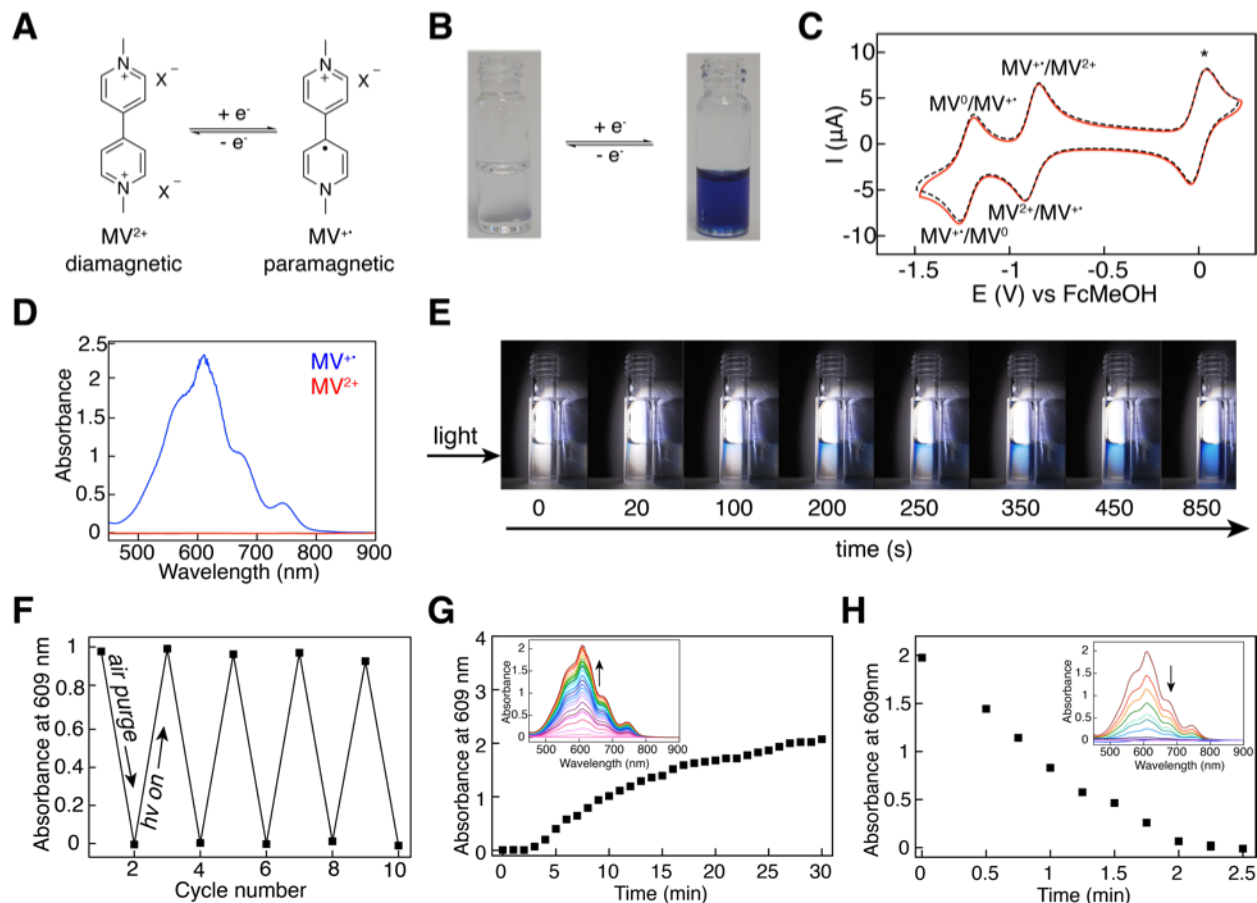


Figure 1: Summary of electrochemical, chemical and photochemical redox behaviour of MV in an example DES, ChCl-glycerol. (A) Structural representation of the redox behaviour of MV and changes in magnetic behaviour upon oxidation and reduction. (B) Images of vials showing MV in ChCl-glycerol DES (0.38 mM) in air before and after reduction. (C) Cyclic voltammetry in air of MV in ChCl-glycerol DES (5 mM) showing 2nd cycle (red) and 102nd cycle (black) with FcMeOH as an internal standard. *Denotes the FcMeOH $^+$ /FcMeOH couple (glassy carbon working electrode, $v = 100 \text{ mV s}^{-1}$, 40°C). (D) UV/vis spectra of MV^{2+} in ChCl-glycerol DES (0.39 mM) upon addition of a reducing agent (monoethanolamine) to form $MV^{+•}$ (blue) and following purging with air (red). (E) Photographs depicting the growth of $MV^{+•}$ species (blue) at the interface between the solution and the incident light with time (see Supporting Video S1). (F) Photochromic cycling behaviour between MV^{2+} and $MV^{+•}$ in ChCl-glycerol DES. Cycles consisted of photoirradiation with solar light simulator for 5 min following by purging with air for 5 min repeated over multiple cycles. (G) UV/vis spectra showing the formation of $MV^{+•}$ from photoirradiation of MV^{2+} (3.8 mM) in ChCl-glycerol DES with time. (H) UV/vis spectra showing the oxidation of $MV^{+•}$ formed in (G) to MV^{2+} through purging with air (30 mL min $^{-1}$).

Thermal switching. In order to employ heat as a stimulus, we made use of a thermal phenomenon unique to ChCl-urea DES. Thermochromism was studied by monitoring the UV/vis spectrum of a solution of MV^{2+} in ChCl-urea DES as a function of temperature (Fig. S8). Heating to 130 °C for 30 min in air resulted in a blue solution with characteristic absorbances at $\lambda = 399$ and 609 nm, consistent with the formation of $MV^{+\cdot}$ (Fig. 2A). The presence of the paramagnetic $MV^{+\cdot}$ radical was further corroborated by EPR spectroscopy. At 80 °C the solution was EPR-silent (Fig. S9A) however, upon heating to 130 °C, a strong EPR signal appeared (Fig. 2B, $g = 2.0023$) indicative of the paramagnetic $MV^{+\cdot}$ radical cation.^{18,19} Control spectra of ChCl-urea DES heated to 130 °C in the absence of MV^{2+} (Fig. S9B) were found to be EPR-silent showing the paramagnetic species is not a result of solvent degradation. Moreover, the EPR spectra of the thermally reduced MV^{2+} was analogous to that of a chemically reduced species, Fig. S9C. Radical formation was similarly observed in other DES when a catalytic amount of urea was added.

Detailed mass spectrometry (MS) and gas-phase infrared spectroscopy (IR) experiments were carried out to elucidate the mechanism. In both the MS and IR spectra the formation of NH_3 (≈ 2.6 mM) was observed upon heating ChCl-urea DES to 100 °C (Fig. 2C, S10-11). Upon further heating to 130 °C, NH_3 was still observed (≈ 30 mM), however, in both the IR and MS spectra (Fig. 2D, S12) additional peaks appeared, which were identified as trimethylamine (TMA, (≈ 2 mM)) (Fig. 2D, S13). This suggested that NH_3 was involved in the formation of TMA.

To further probe the underlying mechanism, four deuterated DES variants were prepared. These had either no deuteration (HH-DES), deuteration of ChCl (DH-DES), deuteration of urea (HD-DES) or deuteration of both components (DD-DES). Through heating these series of deuterated

DES mixtures, the NH_3 produced was shown to originate from the urea component as no difference was observed between the MS spectra of HH-DES and DH-DES, whereas HD-DES and DD-DES showed an additional peak at $m/z = 20$ corresponding to ND_3 , Fig. S12. TMA was shown to arise from the ChCl component, the predominant peak at $m/z = 58$ ($\text{N}(\text{CH}_3)_3$) was shifted to $m/z = 67$ in both DH-DES and DD-DES indicating the formation of $\text{N}(\text{CD}_3)_3$, Fig. S12. It is likely that smaller quantities of dimethylamine and methylamine are also formed, however, they are masked by the TMA fragmentation.

The proposed cycle (Fig. 2E) is initiated by the generation of NH_3 at $100\text{ }^\circ\text{C}$ from condensation of urea to form biuret.⁴⁰ Upon increasing the temperature to $130\text{ }^\circ\text{C}$, NH_3 reacts with ChCl to form TMA and monoethanolamine (MEA, not observed in the gas phase due to its low vapour pressure), which is a known reducing agent.^{41,42} UV/vis studies confirmed that adding MEA to MV^{2+} results in the formation of $\text{MV}^{+\cdot}$ (Fig. S14) whereas adding NH_3 and TMA did not (Fig. S15, S16). Serendipitously, the reaction of MEA with MV^{2+} forms $\text{MV}^{+\cdot}$ regenerating NH_3 .^{41,42} The cycle (Fig. 2E) shows how both ChCl and urea DES components play key roles. Using a deuterated MV isotopologue, $d_6\text{-MV}^{2+}$, showed no change in the MS and thus, any potential role of MV^{2+} itself in the reduction pathway was ruled out (Fig. S17).

Thermal mediated reduction had not been previously reported therefore this new stimuli was tested for another class of radical species, perylene bis(diimides) (PDI), Fig. S18. Heating a solution of PDI in ChCl -urea DES to $130\text{ }^\circ\text{C}$ resulted in analogous thermal reduction to that observed for MV, forming a radical species evidenced by UV/Vis and EPR spectroscopies, Fig. S19. The EPR spectrum was analogous to that of a PDI radical formed from chemical reduction, Fig. S20.

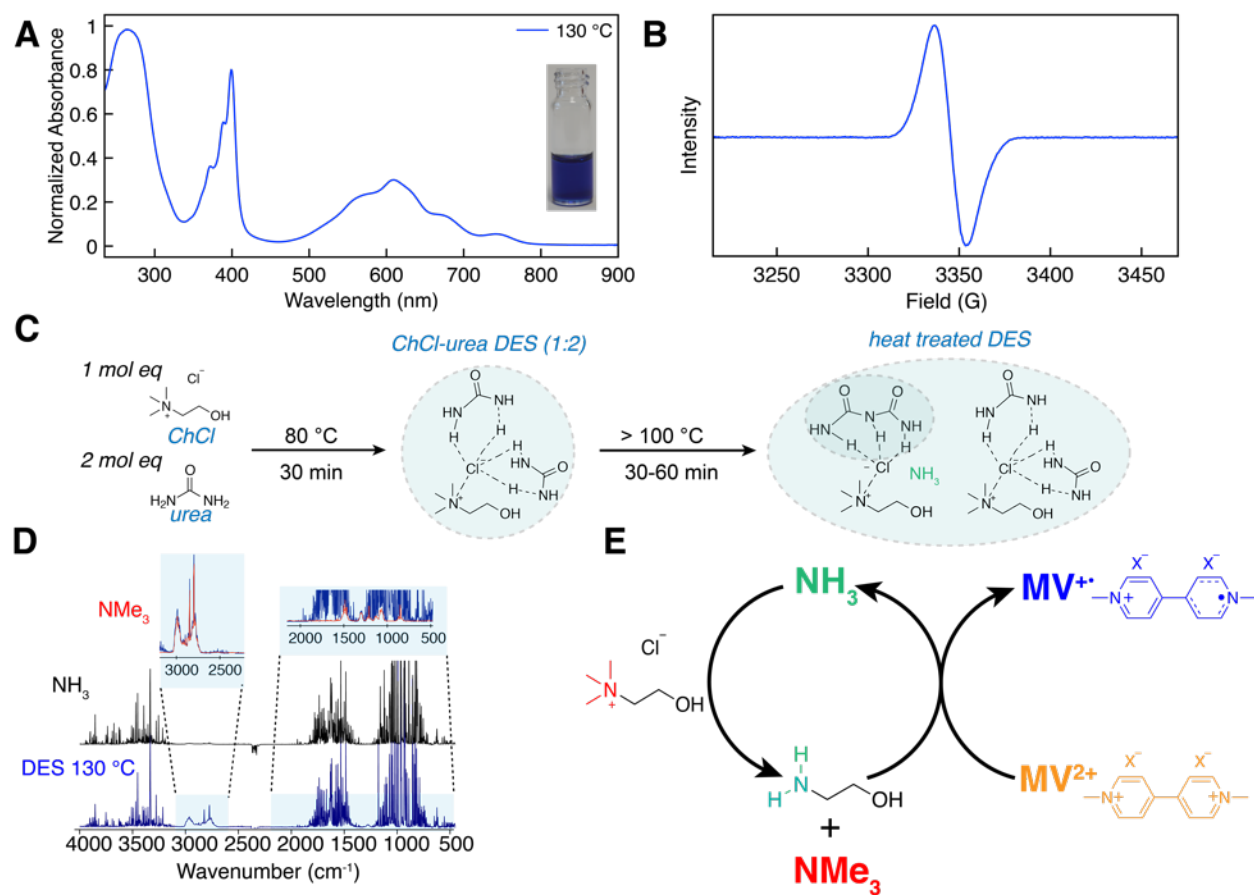


Figure 2: Thermal switching of MV in ChCl-urea DES. (A) UV/vis spectra of $MV^{+•}$ in ChCl-urea DES following heating of MV^{2+} solution to 130 °C. Spectrum shows characteristic λ_{max} =399, 609 nm (inset: photo of $MV^{+•}$ solution). (B) EPR spectrum of $MV^{+•}$ in ChCl-urea DES (1 mM) formed through thermal stimulus. (C) Schematic depicting the formation of DES and structural changes following thermal treatment. (D) Gas-phase IR spectra of ChCl-urea DES heated to 130 °C (blue), reference spectrum of NH_3 (black). Zoom inset shows 2500–3000 cm^{-1} and 2000–1000 cm^{-1} regions, heated DES (blue) and NMe_3 reference (red). (E) Proposed mechanism for MV^{2+} reduction induced within ChCl-urea DES upon introduction of a thermal stimulus.

Long-lived nature of the radical species. Quenching of $MV^{+\cdot}$ occurs through reaction with oxygen and typically happens readily in the liquid and solid state upon exposure to air. However, throughout all experiments we observed that the radical species was remarkably persistent under aerobic conditions. To probe the lifetime of the radical in air, a solution of $MV^{+\cdot}$ in ChCl-urea DES was exposed to air and UV/vis spectra were recorded over a 100 h period (Fig. 3A). The solution was not degassed nor was any attempt to minimise oxygen made however, remarkably, the solution showed no change in absorbance at 609 nm during this time-period. Solutions prepared and stored in air were found to remain blue for > 6 months and thus we forecast a lifetime of >> 6 months for $MV^{+\cdot}$ in DES. The persistence of the radical in the DES environment despite exposure to air suggested that oxygen diffusivity was minute. A time-lapse video of $MV^{+\cdot}$ in DES (Supporting Video S2) showed the solution turning colourless at the interface whilst the bulk remained blue for over a month. This indicated that oxygen was able to permeate the solution and quench the radical but on a much slower time scale than is observed in any other solvents (weeks vs. seconds).

The low oxygen diffusivity into the DES is a contributing factor to the long radical lifetime, however, it was unclear how stable the radical would be when introduced into an oxygenated environment or when oxygen was forced into the DES environment. As shown in Fig. 3B, when a solution of $MV^{+\cdot}$ was poured into air-saturated water the radical persisted in the DES solution. The unique nanostructure of the DES shielded the radical species from interaction with oxygen in the water and thus, a blue solution of $MV^{+\cdot}$ in DES was present at the bottom of the flask. The blue colour remained until complete mixing of the two solutions had occurred. The persistence of the radical was also observed when water was added to a DES $MV^{+\cdot}$ solution (Supporting Video S3).

To demonstrate the stabilisation of $MV^{+\cdot}$ in DES *vs.* water, oxygen was forced into the system by purging aqueous and DES $MV^{+\cdot}$ solutions with air (30 mL min^{-1}) and recording UV/vis spectra in parallel to monitor the quenching of $MV^{+\cdot}$ (Fig. 3C). It was necessary to degas the aqueous $MV^{+\cdot}$ solution and seal it under a N_2 atmosphere as, in air, the radical species did not persist long enough for any measurements to be taken. In contrast, the DES solution was not degassed or sealed. Within less than 4 min of purging with air (0.1 mL min^{-1}), the aqueous $MV^{+\cdot}$ solution was completely quenched, however, in DES under more extreme purging conditions (30 mL min^{-1}), the radical species persisted for 2–15 h, an enhancement factor of approximately 10^5 . The prolonged radical lifetime was not found to be dependent on the viscosity of the DES. Whilst the DES with the lowest viscosity, ChCl-ethylene glycol (36 cP),²⁶ did result in the shortest radical lifetime upon purging with air (Fig. 3C) the $MV^{+\cdot}$ was found to be significantly more persistent in a DES of medium viscosity, ChCl-glycerol (376 cP),²⁶ with a lifetime more than double (900 *vs.* 400 min) that of the more viscous ChCl-urea DES (632 cP).²⁶ These findings suggest that stabilisation of the radical species arises from a number of different factors notably, not simply oxygen diffusivity. The non-linear relationship between viscosity and lifetime indicate that the stabilisation of the radical species arises from factors other than the diffusivity of oxygen into the DES which would be controlled by viscosity. The stabilisation likely arises from a combination of different factors including poor solubility of oxygen in DES (See Supporting Information) and the unique DES nanostructure and the interactions between the radical and the solvent, which shield the species from oxygen present in the surrounding environment. In this case, the nature of the hydrogen bond donor component (alcohol *vs.* amide) was found to play a role. To further probe the solvent–

radical interactions that are responsible for stabilisation, extensive neutron scattering experiments were carried out, which have only revealed information on the bulk solvent properties.⁴³

Application towards fabrication of a smart-window. The redox behaviour of MV has been exploited in the development of electrochromic devices such as displays, mirrors and smart windows by many industry leaders because of the high optical contrast between the MV^{2+} and $MV^{+\cdot}$ states. Typically, this requires chemical modification, immobilisation, encapsulation or incorporation into a nanomaterial to prevent bleaching of the $MV^{+\cdot}$ state. In contrast, the $MV^{+\cdot}$ radical is ultrastable in DES without any costly modifications and the electrochemistry of unmodified MV^{2+} was found to be completely reversible and stable over 100 cycles in air (*vide supra*). Moreover, the DES can act as an electrolyte itself and all components are cheap, non-toxic and biodegradable thus making this system ideal for the fabrication of an electrochromic device (Fig. 4). Unique to this system there are four different stimuli that can be used to modulate the colour unlike current chromic devices which typically use only one.

A simple device was constructed consisting of two pieces of fluorine-doped tin oxide (FTO) separated by a membrane with ChCl-ethylene glycol DES on one side and the same DES with MV^{2+} on the other (Fig. 4A). Upon application of a negative bias (-3V) between the two electrodes, the device reversibly changed from colourless to blue. This colour was found to be stable even when the bias was removed (Fig. 4B) and only when a positive bias (+3 V) was applied did the device revert to the colourless state (Fig. 4C). Application of a negative bias (-3 V) led to an increase in the absorbance at 609 nm indicative of the formation of $MV^{+\cdot}$ whilst application of a positive bias resulted in a decrease in absorbance at 609 nm confirming reoxidation to MV^{2+} . Switching

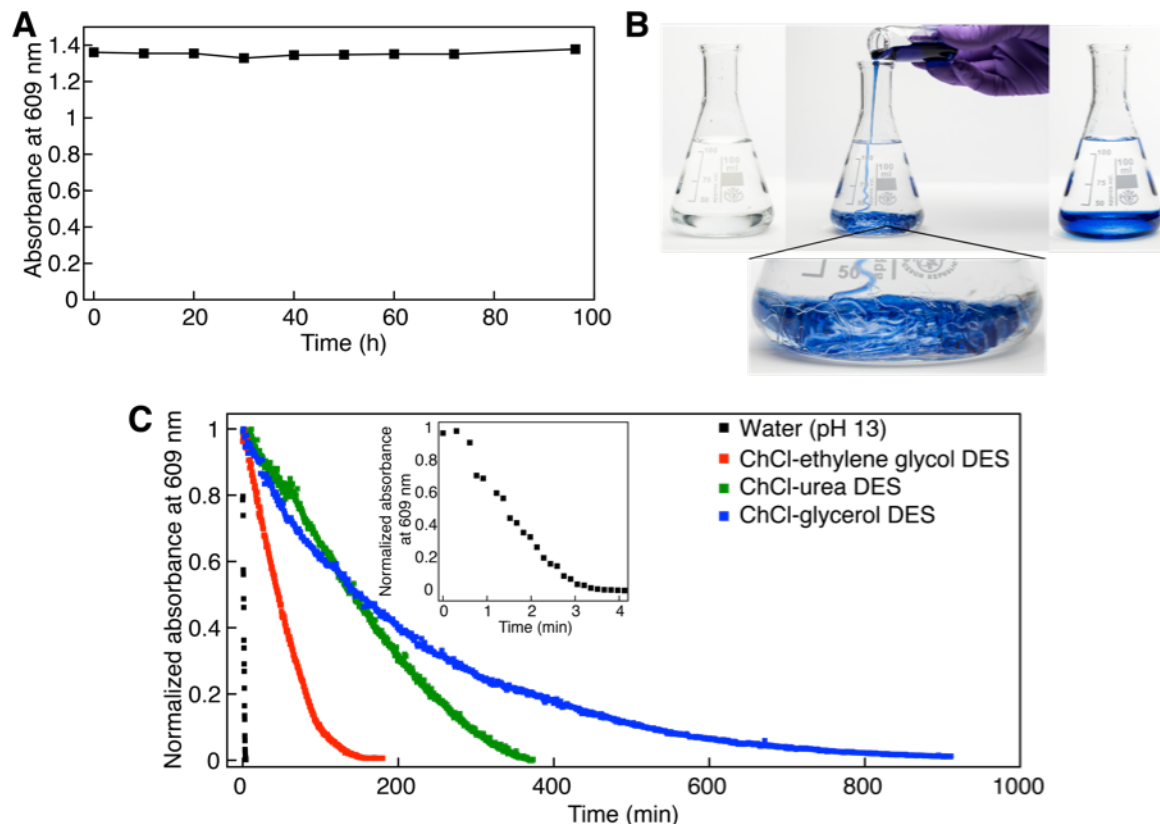


Figure 3: Stability of $MV^{+\bullet}$ species in DES under aerobic conditions. (A) Long-term UV/vis measurement of $MV^{+\bullet}$ in ChCl-urea DES (0.39 mM). Spectra recorded over a 100 h period with no change in absorbance. (B) Images showing a solution of $MV^{+\bullet}$ in ChCl-urea DES being poured into air-saturated water highlighting how the DES structure is protecting the radical from O_2 . The solution remained blue until complete mixing had occurred and the DES nanostructure was destroyed. (C) Overview of the stability of $MV^{+\bullet}$ in three different DES and comparison to water (pH 13). Solutions of $MV^{+\bullet}$ were prepared by chemical reduction (MEA, 90.6 μ L) and reoxidation as a function of time was measured through continuous acquisition of UV/vis spectra whilst purging with air (for DES 30 ml min⁻¹ for water (pH 13) 0.1 mL min⁻¹).

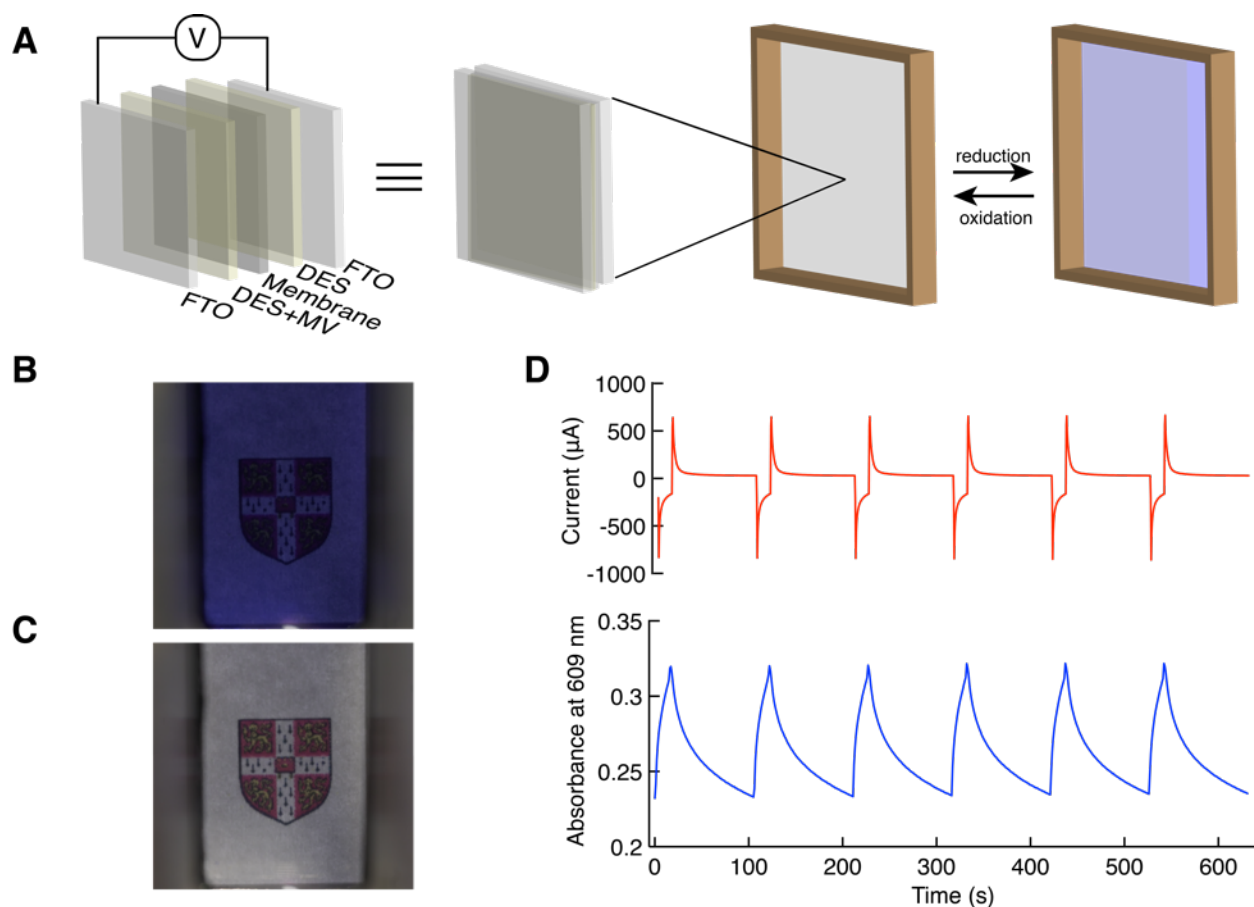


Figure 4: Fabrication and performance of a 'smart window' based on MV in DES. (A) Illustration of a 'smart window' showing the colour modulation with application of bias. (B) Schematic representation of the electrochromic device showing the components involved and the set up. (C) Photographs of the 'smart window' upon application of a reductive bias (-3 V, 15 s) and (D) oxidative bias (-3 V, 90 s). (E) Electrochemical switching of the 'smart window' showing the alternating bias applied (top) and resultant change in absorbance at 609 nm monitored by UV/vis spectroscopy (bottom) over multiple cycles.

behaviour of the device was rapid and robust, and the device could undergo multiple switching cycles without bleaching, precipitation or loss in performance (Fig. 4D). The use of DES thus allows for a highly desirable low-cost device construction using only inexpensive and widely available components, namely ChCl (chicken feed), urea (produced on a multi-ton scale) and MV (common herbicide). Its robust nature and excellent performance leads us to believe that this technology holds significant potential in electrochromic applications.

Conclusions The formation of $MV^{+\cdot}$ in various DES has been shown using an electrochemical, chemical, photochemical and, for ChCl-urea DES, a unique thermal stimulus. Typically, organic radicals such as $MV^{+\cdot}$ are known to be unstable, rapidly quenched upon exposure to oxygen present in air, however, in DES we found the radical to be extremely stable under aerobic conditions with a projected lifetime of over 6 months. The stability is a specific feature of DES, arising from the unique chemical environment provided by the liquid nanostructure which protects the radical species from atmospheric oxygen. This supramolecular solvation shielding phenomenon allowed the lifetime of $MV^{+\cdot}$ in air to be extended without altering the electronic or chemical structure of the molecule. Access to a persistent, air-stable, redox responsive radical in DES signifies a step-change in the chemistry of highly reactive chemical species unveiling a new methodology for taming these, and undoubtedly other, moieties in air. The use of viologens in electrochromic devices including ‘smart-windows’ has been impeded in the past by poor write-erase efficiencies and rapid bleaching in air requiring the development of derivatised materials. The air-stable $MV^{+\cdot}$ in DES was found to be applicable in the fabrication of a smart window through cheap, solution based methodology. The window fabricated was inexpensive, robust and responsive to multiple

different stimuli offering a new approach to the design and construction of cost-effective switchable devices for next-generation nanotechnology.

Author Contributions Conceptualisation, J.A.M.; Methodology, J.A.M. and M.F.K.; Investigation, J.A.M. and M.F.K.; Writing—original draft - J.A.M.; Writing—Review & Editing, J.A.M., M.F.K., E.R. and O.A.S.; Funding Acquisition E.R. and O.A.S.; Resources E.R. and O.A.S.; Supervision, E.R. and O.A.S.

Declaration of Interests The authors declare no competing interests.

1. Fukino, T., Yamagishi, H. & Aida, T. Redox-responsive molecular systems and materials. *Adv. Mater.* **29**, 1603888–17 (2016).
2. Li, Z., Barnes, J. C., Bosoy, A., Stoddart, J. F. & Zink, J. I. Mesoporous silica nanoparticles in biomedical applications. *Chem. Soc. Rev.* **41**, 2590–17 (2012).
3. Thakur, V. K., Ding, G., Ma, J., Lee, P. S. & Lu, X. Hybrid materials and polymer electrolytes for electrochromic device applications. *Adv. Mater.* **24**, 4071–4096 (2012).
4. Lin, W.-P., Liu, S.-J., Gong, T., Zhao, Q. & Huang, W. Polymer-based resistive memory materials and devices. *Adv. Mater.* **26**, 570–606 (2013).
5. Kim, D. J. *et al.* Redox-active macrocycles for organic rechargeable batteries. *J. Am. Chem. Soc.* **139**, 6635–6643 (2017).

6. Cram, D. J., Tanner, M. E. & Thomas, R. The taming of cyclobutadiene. *Angew. Chem. Int. Ed.* **30**, 1024–1027 (1991).
7. Mal, P., Breiner, B., Rissanen, K. & Nitschke, J. R. White phosphorus is air-stable within a self-assembled tetrahedral capsule. *Science* **324**, 1697–1699 (2009).
8. Lopez, N. *et al.* Reversible reduction of oxygen to peroxide facilitated by molecular recognition. *Science* **335**, 450–453 (2012).
9. Jiao, Y. *et al.* A supramolecularly activated radical cation for accelerated catalytic oxidation. *Angew. Chem. Int. Ed.* **55**, 8933–8937 (2016).
10. Benson, C. R. *et al.* Extreme stabilization and redox switching of organic anions and radical anions by large-cavity, CH hydrogen-bonding cyanostar macrocycles. *J. Am. Chem. Soc.* **138**, 15057–15065 (2016).
11. Song, Q., Li, F., Wang, Z. & Zhang, X. A supramolecular strategy for tuning the energy level of naphthalenediimide: Promoted formation of radical anions with extraordinary stability. *Chem. Sci.* **6**, 3342–3346 (2015).
12. Ghosh, I., Ghosh, T., Bardagi, J. I. & König, B. Reduction of aryl halides by consecutive visible light-induced electron transfer processes. *Science* **346**, 725–728 (2014).
13. Monk, P. M. S., Rosseinsky, D. R. & Mortimer, R. J. *Electrochromic materials and devices based on viologens*, 57–90 (Wiley-VCH Verlag GmbH & Co. KGaA, 2013).

14. Sweetser, P. B. Colorimetric determination of trace levels of oxygen in gases with the photochemically generated methyl viologen radical-cation. *Anal. Chem.* **39**, 979–982 (1967).
15. Jeon, W. S., Kim, H.-J., Lee, C. & Kim, K. Control of the stoichiometry in host–guest complexation by redox chemistry of guests: Inclusion of methylviologen in cucurbit[8]uril. *Chem. Commun.* 1828–1829 (2002).
16. Kim, H.-J., Jeon, W. S., Ko, Y. H. & Kim, K. Inclusion of methylviologen in cucurbit[7]uril. *Proc. Natl. Acad. Sci. U.S.A.* **99**, 5007–5011 (2002).
17. Zhang, L. *et al.* A two-dimensional single-layer supramolecular organic framework that is driven by viologen radical cation dimerization and further promoted by cucurbit[8]uril. *Polym. Chem.* **5**, 4715–4721 (2014).
18. Fiala, T. *et al.* Bambusuril as a one-electron donor for photoinduced electron transfer to methyl viologen in mixed crystals. *J. Am. Chem. Soc.* **139**, 2597–2603 (2017).
19. Wu, J., Tao, C., Li, Y., Li, J. & Yu, J. Methyl viologen-templated zinc gallophosphate zeolitic material with dual photo-/thermochromism and tuneable photovoltaic activity. *Chem. Sci.* **6**, 2922–2927 (2015).
20. Odell, B. *et al.* Cyclobis(paraquat-p-phenylene). a tetracationic multipurpose receptor. *Angew. Chem., Int. Ed.* **27**, 1547–1550 (1988).
21. Trabolsi, A. *et al.* Radically enhanced molecular recognition. *Nat. Chem.* **2**, 42–49 (2009).
22. Barnes, J. C. *et al.* A radically configurable six-state compound. *Science* **339**, 429–433 (2013).

23. Barnes, J. C. *et al.* Solid-state characterization and photoinduced intramolecular electron transfer in a nanoconfined octacationic homo[2]catenane. *J. Am. Chem. Soc.* **136**, 10569–10572 (2014).
24. Abbott, A. P., Capper, G., Davies, D. L., Rasheed, R. K. & Tambyrajah, V. Novel solvent properties of choline chloride/urea mixtures. *Chem. Commun.* **0**, 70–71 (2002).
25. Abbott, A. P., Boothby, D., Capper, G., Davies, D. L. & Rasheed, R. K. Deep eutectic solvents formed between choline chloride and carboxylic acids: Versatile alternatives to ionic liquids. *J. Am. Chem. Soc.* **126**, 9142–9147 (2004).
26. Smith, E. L., Abbott, A. P. & Ryder, K. S. Deep eutectic solvents (DESs) and their applications. *Chem. Rev.* **114**, 11060–11082 (2014).
27. Zhang, Q., De Oliveira Vigier, K., Royer, S. & Jérôme, F. Deep eutectic solvents: syntheses, properties and applications. *Chem. Soc. Rev.* **41**, 7108–39 (2012).
28. Hammond, O. S., Bowron, D. T. & Edler, K. J. Liquid structure of the choline chloride-urea deep eutectic solvent (reline) from neutron diffraction and atomistic modelling. *Green Chem.* **18**, 2736–2744 (2016).
29. Ashworth, C. R., Matthews, R. P., Welton, T. & Hunt, P. A. Doubly ionic hydrogen bond interactions within the choline chloride-urea deep eutectic solvent. *Phys. Chem. Chem. Phys.* **18**, 18145–18160 (2016).

30. Hammond, O. S., Bowron, D. T. & Edler, K. J. The effect of water upon deep eutectic solvent nanostructure: An unusual transition from ionic mixture to aqueous solution. *Angew. Chem. Int. Ed.* **52**, 3074–5 (2017).
31. Abbott, A. P., Nandhra, S., Postlethwaite, S., Smith, E. L. & Ryder, K. S. Electroless deposition of metallic silver from a choline chloride-based ionic liquid: a study using acoustic impedance spectroscopy, SEM and atomic force microscopy. *Phys. Chem. Chem. Phys.* **9**, 3735–9 (2007).
32. Liao, H.-G., Jiang, Y.-X., Zhou, Z.-Y., Chen, S.-P. & Sun, S.-G. Shape-controlled synthesis of gold nanoparticles in deep eutectic solvents for studies of structure-functionality relationships in electrocatalysis. *Angew. Chem. Int. Ed.* **47**, 9100–9103 (2008).
33. García, G., Aparicio, S., Ullah, R. & Atilhan, M. Deep eutectic solvents: Physicochemical properties and gas separation applications. *Energy Fuels* **29**, 2616–2644 (2015).
34. Alonso, D. A. *et al.* Deep eutectic solvents: The organic reaction medium of the century. *Eur. J. Org. Chem.* **2016**, 612–632 (2016).
35. Vidal, C., García-Álvarez, J., Hernán-Gómez, A., Kennedy, A. R. & Hevia, E. Exploiting deep eutectic solvents and organolithium reagent partnerships: Chemoselective ultrafast addition to imines and quinolines under aerobic ambient temperature conditions. *Angew. Chem. Int. Ed.* **128**, 16379–16382 (2016).
36. Cruz, H., Jordão, N. & Branco, L. C. Deep eutectic solvents (DESs) as low-cost and green electrolytes for electrochromic devices. *Green Chem.* **19**, 1653–1658 (2017).

37. Ebbesen, T. W., Levey, G. & Patterson, L. K. Photoreduction of methyl viologen in aqueous neutral solution without additives. *Nature* **298**, 545–548 (1982).
38. Xu, G. *et al.* Photochromism of a methyl viologen Bismuth(III) chloride: Structural variation before and after UV irradiation. *Angew. Chem. Int. Ed.* **46**, 3249–3251 (2007).
39. Peon, J. *et al.* Excited state dynamics of methyl viologen. ultrafast photoreduction in methanol and fluorescence in acetonitrile. *J. Phys. Chem. A* **105**, 5768–5777 (2001).
40. Redemann, C. E., Riesenfeld, F. C. & Viola, F. S. L. Formation of biuret from urea. *Ind. Eng. Chem. Res.* **50**, 633–636 (1958).
41. Meltsner, M., Wohlberg, C. & Kleiner, M. J. Reduction of organic compounds by ethanolamines. *J. Am. Chem. Soc.* **57**, 2554–2554 (1935).
42. Kremer, C. B. & Kress, B. Alkanolamines. IV. Reducing properties of the amino alcohols. *J. Am. Chem. Soc.* **60**, 1031–1032 (1938).
43. Gilmore, M. *et al.* A comparison of choline:urea and choline:oxalic acid deep eutectic solvents at 338 K. *J. Chem. Phys* **148**, 193823 (2018).

Acknowledgements J.A.M. would like to acknowledge the EPSRC for a PhD studentship (EP/K503009/1). O.A.S. acknowledges ERC Consolidator grant CAM-RIG (No.726470) and UK Engineering and Physical Sciences Research Council grant EP/L027151/1. M.F.K. and E.R. acknowledge Christian Doppler Research Association (Austrian Federal Ministry of Science, Research and Economy and the National Foundation

for Research, Technology and Development), the OMV Group and the EPSRC (IAA Follow-on Fund). We thank Mr Sam Schott for his assistance with EPR measurements.

Correspondence Correspondence and requests for materials should be addressed to Oren A. Scherman (email: oas23@cam.ac.uk).